

COMPUTATION AND MODELING OF AERO-THERMAL FIELDS IN TURBINE CASCADES AND STRONGLY CURVED DUCTS

J. Luo and B. Lakshminarayana
Dept. of Aerospace Engineering
The Pennsylvania State University

SUMMARY

Advanced turbulence models are crucial for accurate prediction of rocket engine flows, due to existence of very large extra strain rates, such as strong streamline curvature. Numerical simulation of the turbulent flow in a strongly curved turn-around duct (TAD) has been carried out with a Reynolds stress model (RSM), an algebraic Reynolds stress model (ARSM) and a k - ϵ model. The RSM model and the ARSM model are found to capture the turbulence damping due to the convex curvature, but underpredict the turbulence enhancement caused by the concave curvature. To capture the concave curvature effects, it is necessary to modify the ϵ -equation. The modification of ϵ equation suggested by Launder et al. provides the correct trend, but over-corrects the curvature effects.

A comparative study of two modes of transition in gas turbine, the by-pass transition and the separation-induced transition, has been carried out with several low-Reynolds-number (LRN) k - ϵ models. Effects of blade surface pressure gradient, freestream turbulence and Reynolds number on the blade boundary layer development, and particularly the inception of transition are examined in detail. The present study indicates that the turbine blade transition, in the presence of high freestream turbulence, is predicted well with LRN k - ϵ models employed.

DISCUSSION

Although considerable research has been carried out to model curved turbulent shear flows, most of them deal with mildly curved flows. Previous computation of strongly curved flows, e.g., the turn-around-duct (TAD) flow of Monson et al. (1990), indicated the need for improved turbulence models. Since most turbulence models have been developed using the data for simple shear layers in local equilibrium, they are not accurate for non-equilibrium flows, such as strongly curved flows. The objective of the present work is to develop turbulence models for flows with strong streamline curvature. A secondary objective is to study the effect of transition on turbine flowfield and heat transfer.

Various eddy-viscosity models have been used in previous computations of the TAD flow. In the present investigation, a low-Reynolds-number Reynolds stress model (RSM), developed by Shima (1988) on the basis of the RSM model due to Launder et al. (1975), is employed. The transport equation for Reynolds stress components is given by,

$$\begin{aligned}
\frac{D\overline{u_i u_j}}{Dt} &= \underbrace{-\overline{u_i u_k} U_{j,k} - \overline{u_j u_k} U_{i,k}}_{\text{Convection}} + \underbrace{\frac{p}{\rho} \left(\frac{\partial u_i}{\partial x_j} + \frac{\partial u_j}{\partial x_i} \right)}_{\text{Production}} \\
&\quad - \underbrace{\frac{\partial}{\partial x_k} \left[\overline{u_i u_j u_k} + \frac{p u_j}{\rho} \delta_{ik} + \frac{p u_i}{\rho} \delta_{jk} - v \frac{\partial \overline{u_i u_j}}{\partial x_k} \right]}_{\text{Diffusion}} - \underbrace{2\nu \frac{\partial u_i}{\partial x_k} \frac{\partial u_j}{\partial x_k}}_{\text{Dissipation}}
\end{aligned}$$

where $\overline{u_i u_j}$ is Reynolds stress tensor, and U_i is mean velocity component. The RSM model has one obvious advantage over the eddy-viscosity model since the production term is exact. The modeling of the pressure-strain correlation enables the RSM model to capture the anisotropy of turbulence. The formulations for the above terms are given by Launder et al. (1975) and Shima (1988) and have been incorporated into the Navier-Stokes code.

The details of the present 2-D Navier-Stokes procedure can be found in Luo & Lakshminarayana (1993). The transport equations for individual Reynolds stresses $-\overline{uu}$, $-\overline{vv}$, $-\overline{ww}$ and $-\overline{uv}$ are solved. These equations are discretized in the same way as the k and ϵ equations and are also integrated by the 4-stage Runge-Kutta method. The RSM equations are numerically much stiffer than the eddy-viscosity models. It is necessary to adopt stability enhancing measures, e.g., the normal components of the Reynolds stress tensor are required to be positive during iteration and the Schwarz inequality (i.e., $\overline{u_i u_j}^2 / \overline{u_i^2} \overline{u_j^2} \leq 1.0$) has to be satisfied. A second-order artificial dissipation term is added to the RSM equations to prevent odd-even decoupling, since the convective fluxes are discretized with central differences.

Computation of Turn-Around Duct Flow with Reynolds Stress Model

The prediction for the TAD flow using the RSM model is compared with the data due to Monson et al. (1990). The results obtained by the ARSM and k - ϵ models are also included for comparison. The RSM model successfully captures the turbulence damping effects of convex curvature (inner wall of the duct), but underpredicts the turbulence enhancement caused by strong concave curvature (outer wall), as can be seen from Fig. 1b, 1c, where U_m is the bulk velocity. It has been suggested (e.g, Monson et al.) that the Taylor-Gortler vortices also contribute to the turbulence enhancement in the concave region. However, Barlow & Johnston (1988) found that the turbulence enhancement was due almost entirely to increased energy in large-scale vortices (radial inflows and outflows). They did not observe the Taylor-Gortler vortices. The under-prediction of the turbulence enhancement by all the models (see Fig. 1b & 1c) can be attributed to poor modeling of the source term in the ϵ -equation. Indeed, there is really no reason -- other than convenience and simplicity -- to assume that the influence of mean strain on the spectral transfer of energy from large to small scales is represented by exactly the same interactions between the Reynolds stress and mean velocity gradients as those that generate turbulent kinetic energy (i.e., P_k). The present formulation of the ϵ -equation may work well for cases in local equilibrium ($P_k \approx \epsilon$). For non-equilibrium

flows, such as those in the concave region, the source term in the ϵ -equation should not be so rigidly linked to that of the k -equation. It is known that the viscous dissipation is dominated by small scales, on which the curvature effects are small, while the turbulence energy is generated at large scales, which are greatly influenced by streamline curvature.

Launder et al (1977) modified the destruction term in the ϵ equation to be $-C_{\epsilon 2}(1 - C_c Ri_t)(\epsilon^2/k)$. The Richardson number Ri_t is defined as: $Ri_t = (k^2/\epsilon^2)(U/r^2)(\partial(Ur)/\partial n)$, where r is the curvature radius of streamline, U is the streamwise component of mean velocity, and n is the normal direction. The proposed additional term acts to destroy large eddies (reduce the length scale) in stabilizing curvatures and augment the length scale in destabilizing curvatures. By introducing this curvature modification into the ϵ -equation, all the models captured strong turbulence amplification in the concave region (Figs. 2b & 2c), confirming the above analysis in retrospect. However, this modification is not tensorially invariant, and the curvature effects have been over-corrected. Efforts are underway to improve the modeling of this source term. Specifically, the time scale controlling the spectral energy transfer rate is being modified to capture the differing flow structures in concave and convex curved regions.

Prediction of Turbine Blade Transition and Heat Transfer

An improved understanding and predictive capability of turbine viscous flowfield and heat transfer is crucial in achieving higher turbine performance and efficiency. The mode of transition in gas turbine is bypass transition (in which the 2-D Tollmien-Schlichting instability wave is by-passed) or separated-flow transition. A comparative study of these two modes of transition, on the C3X and Mark II turbine blades (Hylton et al. 1983), has been carried out with three LRN k - ϵ models due to Chien (1982, denoted as CH), Lam-Bremhorst (1981, denoted as LB) and Fan, et al. (1993, denoted as FL), respectively. For both cascades, the downstream Reynolds no. (Re) varied from 1.5×10^6 to 2.5×10^6 , the total temperature (T_0) at the inlet was 700-800 ($^{\circ}k$), and the freestream turbulence intensity (Tu_{∞}) was 6.5% to 8.3%. All parameters are significantly higher than those of the VKI cascade computed by Luo & Lakshminarayana (1993).

The surface pressure (P) distribution and the acceleration factor ($K=(v/U_e^2)dU_e/dS$, U_e is mainstream velocity and S is streamwise distance) distribution are shown in Fig. 3a & 3b, where ARC is total surface distance. For values of K larger than 3.0×10^{-6} (re-laminarization criterion), transition is suppressed for low freestream turbulence, and the turbulent boundary layer begins to re-laminarize. A knowledge of K is thus very useful in understanding turbine boundary layer transition. The prediction of heat transfer, using a 151×99 H-grid, for the Mark II airfoil is presented in Fig. 4a. On the pressure side, all the calculations are in good agreement with the data. On the suction side, the boundary layer (TEXSTAN) calculation is terminated around $S/ARC=0.26$ due to separation, while all the N-S calculations have captured the transition due to separated flow. The transition location as indicated by both the skin friction coefficient (Fig. 4b) and the shape factor (Fig. 4c) is in agreement with the heat transfer distribution. In Fig. 4d, the calculated momentum thickness Reynolds number Re_{θ} on the pressure surface near the trailing edge

reaches only around 500, far below a value of 2000 usually considered as the lower limit for fully turbulent boundary layers, thus suggesting the boundary layer remains transitional along the entire surface.

The calculated heat transfer for the C3X is plotted in Fig. 5a, the performance of various models is similar to that shown in Fig. 4a. As shown in Fig. 5b, the LB model provides an accurate simulation of the transition process in which the velocity profile ($u^+ \sim y^+$) in the outer layer evolves from a laminar boundary layer (linear-law) to that of a fully turbulent boundary layer (log-law). The pressure-gradient effect is examined in Fig. 6. On the suction surface, the increase in local heat transfer rate caused by the separation-induced transition (on Mark II) is much sharper than that caused by nominal by-pass transition (on C3X). For the C3X airfoil, the Reynolds number effect on the heat transfer is reflected in both the transition onset location and general level of heat transfer (see Fig. 7). The higher the Reynolds number, the earlier is the transition, and the higher is the heat transfer rate. The turbulence length scale has significant effect on the predicted suction surface heat transfer near the stagnation point as well as the transition location, as shown in Fig. 8.

It is concluded that the transition on turbine blades with high freestream turbulence can be predicted well with LRN $k-\epsilon$ models, provided that the artificial dissipation is kept minimum. In both measurement and computation, the separation-induced transition leads to much sharper increase of local heat transfer than the nominal by-pass transition. The Lam-Bremhorst's $k-\epsilon$ model provides the best prediction of transition.

ACKNOWLEDGEMENTS

This work was supported by the U.S. National Aeronautics and Space Administration through contract NAS 8-38867 monitored by Lisa Griffin of Marshall Space Flight Center (MSFC). The authors wish to acknowledge NASA for providing the supercomputing resources at NASA MSFC.

REFERENCES

- Barlow, R. S. & Johnston, J. P., 1988, "Structure of a Turbulent Boundary Layer on a Concave Surface," *J. Fluid Mech.*, Vol. 191, p. 137.
- Chien, K. Y., 1982, "Prediction of Channel and Boundary-Layer Flows with a Low-Reynolds Number Turbulence Model," *AIAA Journal*, Vol. 20, No. 1.
- Fan, S., Lakshminarayana, B. and Barnett, M., 1993, "Low-Reynolds-Number $k-\epsilon$ Model for Unsteady Turbulent Boundary-Layer Flows," *AIAA Journal*, Vol. 32, No. 10, pp. 1777-1784.
- Hylton, L. D., Mihelc, M. S., Turner, E. R., Nealy, D. A., and York, R. E., 1983, "Analytical and Experimental Evaluation of the Heat Transfer Distribution Over the Surface of Turbine Vanes," NASA CR-168015, May.
- Lam, C. & Bremhorst, K., 1981, "Modified form of the $k-\epsilon$ Model for Predicting Wall Turbulence," *J. Fluid Engr.*, Vol. 103, P.456.
- Launder, B.E., Reece, G.J. and Rodi, W., 1975, "Progress in the Development of a Reynolds-Stress Turbulence Closure," *J. Fluid Mech.*, Vol. 68, p.537.
- Launder, B., Priddin, C.H. and Sharma, B., 1977, "The Calculation of Turbulent Boundary Layers on Curved and Spinning Surfaces," *ASME J. of Fluids Engr.*, Vol. 98, p.753.
- Luo, J. & Lakshminarayana, B., 1993, "Navier-Stokes Analysis of Turbine Flowfield and Heat Transfer," AIAA 93-7075, ISABE, Tokyo, Japan, to appear on *J. of Propulsion and Power*.
- Monson D. J., Seegmiller, H. L., McConnaughey, P. K. & Chen, Y. S., 1990, "Comparison of Experiment with Calculations Using Curvature-Corrected Zero & Two Equation Turbulence Models for a Two-Dimensional U-Duct," AIAA Paper 90-1484, June.
- Shima, N., 1988, "A Reynolds Stress Model for Near-wall and Low-Reynolds-Number Regions," *J. of Fluids Engr.*, Vol. 110, pp.38-44.

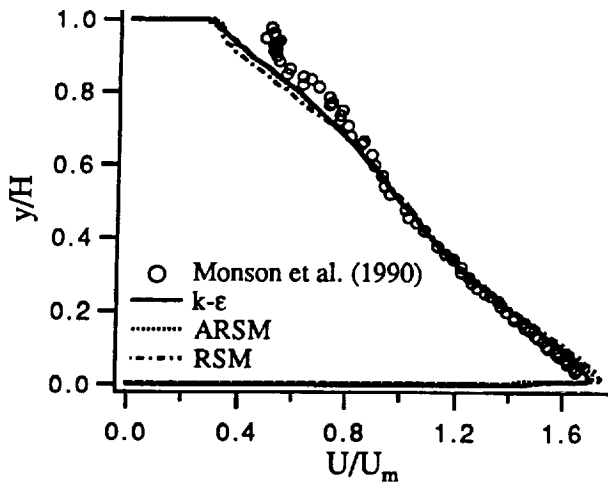


Fig. 1a Longitudinal velocity profile, $\theta=60^\circ$.
(y =normal distance from inner wall, H =duct height).

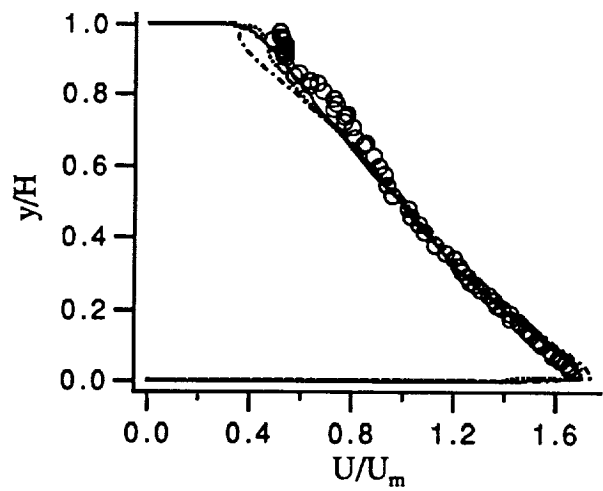


Fig. 2a Longitudinal velocity profile, $\theta=60^\circ$.
(Legend as in Fig. 2b)

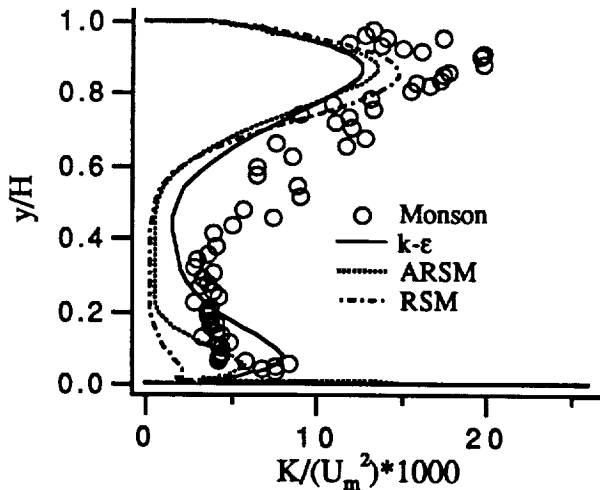


Fig. 1b Turbulent kinetic energy profile.

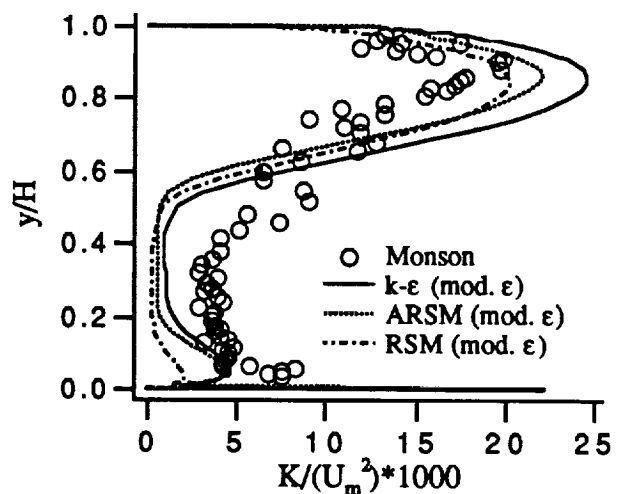


Fig. 2b Turbulent kinetic energy profile.

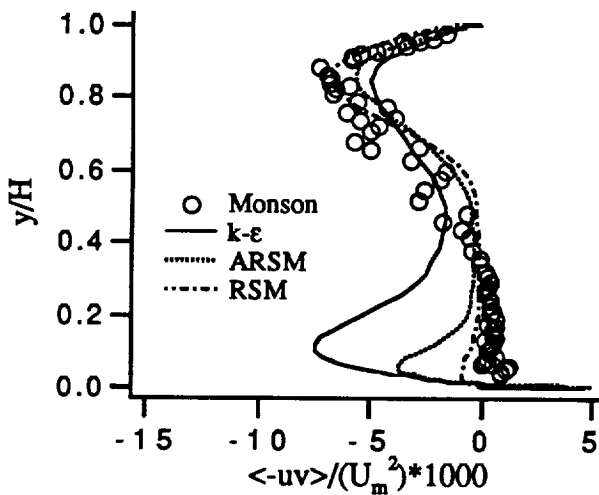


Fig. 1c Turbulent shear stress profile

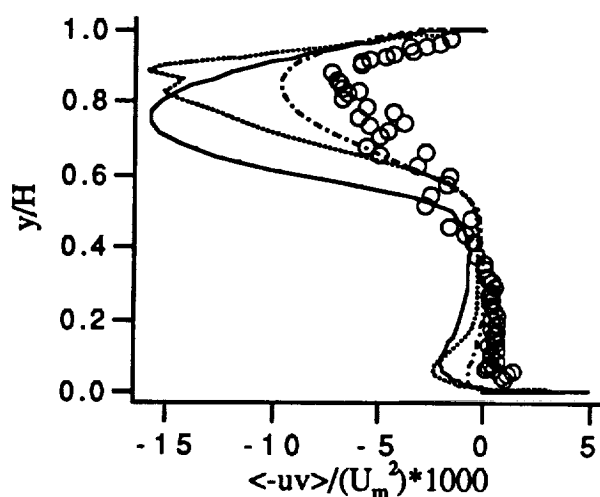


Fig. 2c Turbulent shear stress profile (legend as in Fig. 2b)

(all the above 6 figures are for predictions at $\theta=60^\circ$)

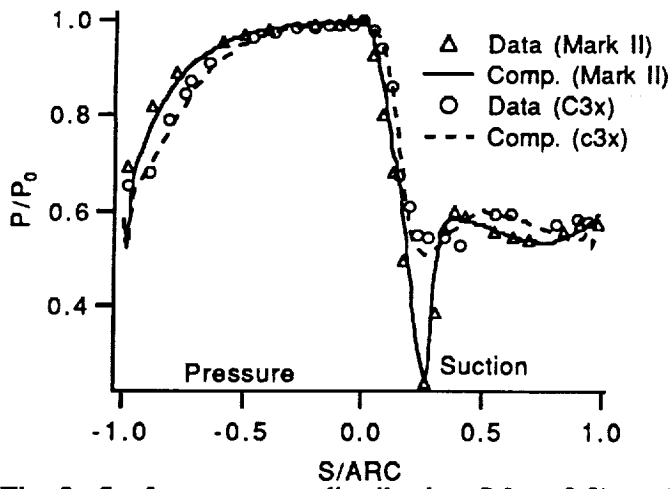


Fig. 3a Surface pressure distribution ($M_{is2}=0.9$)

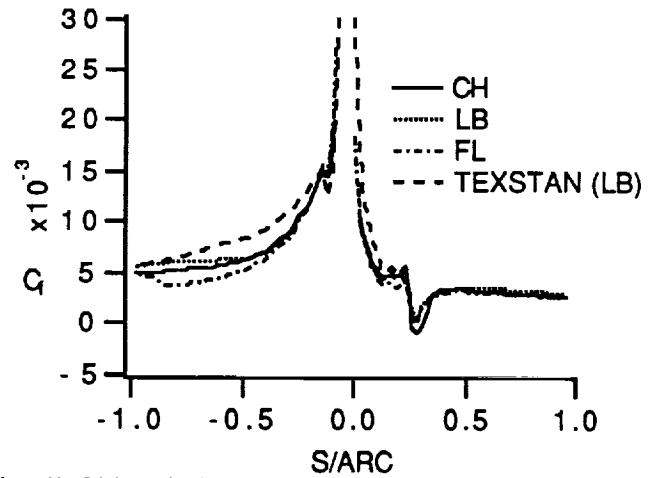


Fig. 4b Skin friction coefficient

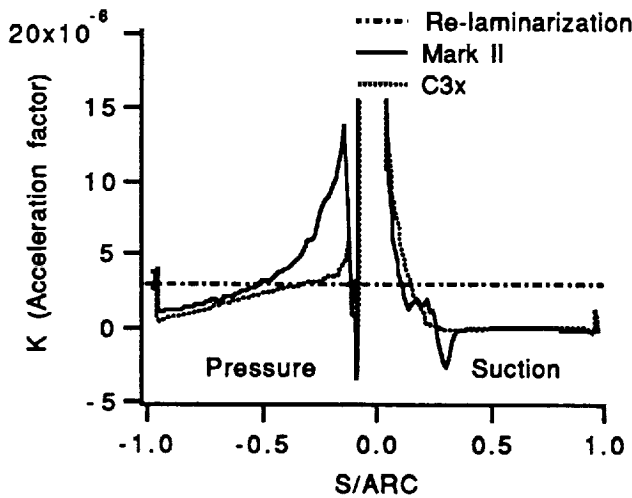


Fig. 3b Acceleration factors for above cases

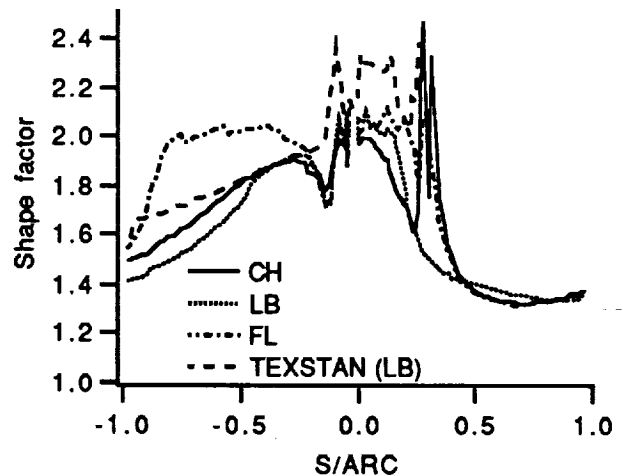


Fig. 4c Blade boundary layer shape factor

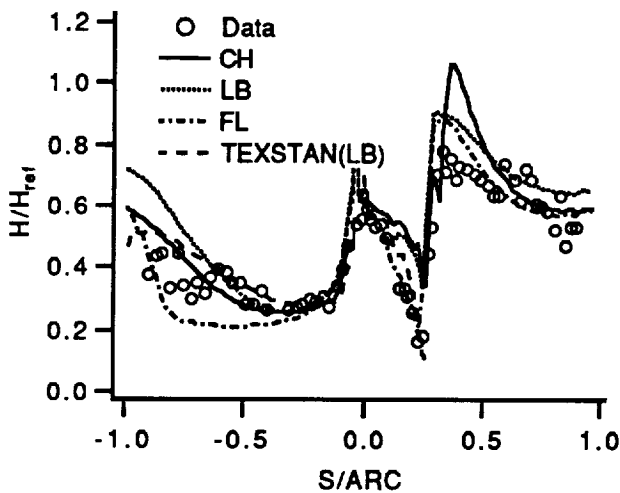


Fig. 4a Heat transfer for Mark II
($M_{is2}=0.90$, $Re_{is2}=1.6 \times 10^6$, $Tu_{\infty}=8.3\%$)

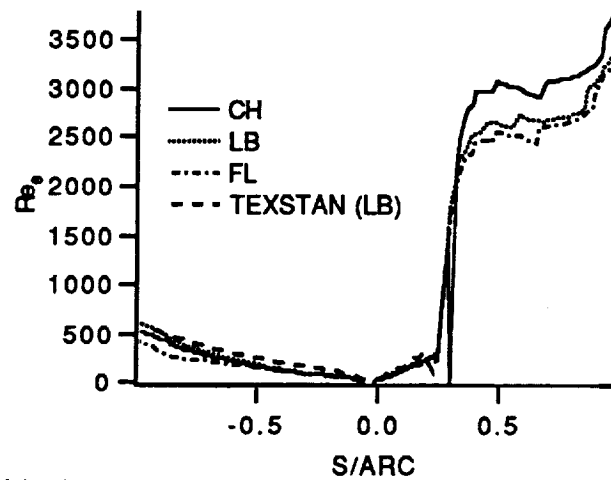


Fig. 4d Momentum thickness Reynolds number

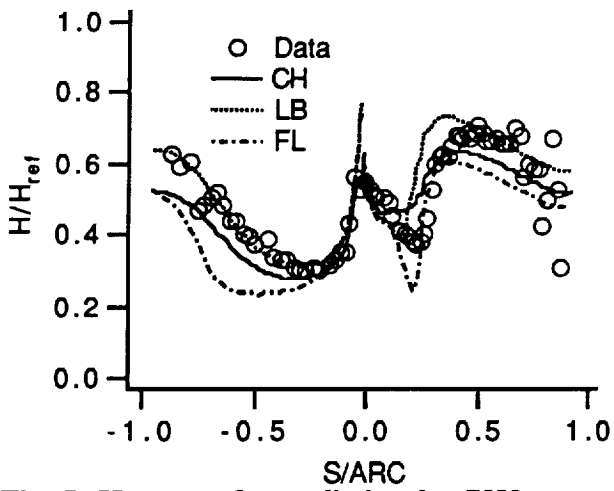


Fig. 5a Heat transfer prediction for C3X.
 ($M_{is2}=0.90$, $Re_{is2}=1.5 \cdot 10^6$, $Tu_{\infty}=8.3\%$)

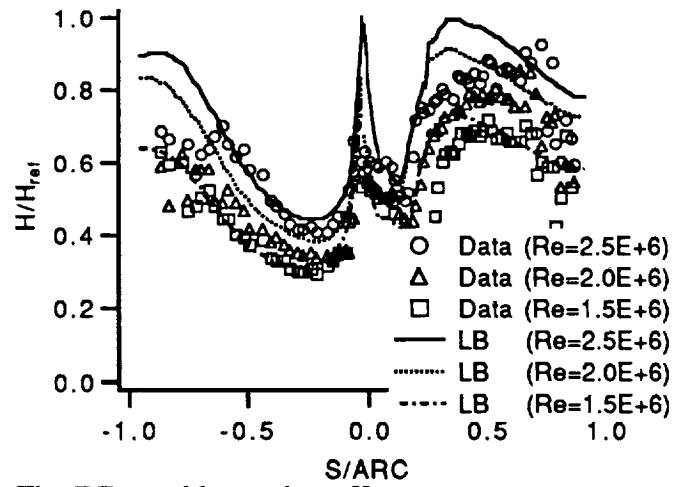


Fig. 7 Reynolds number effect

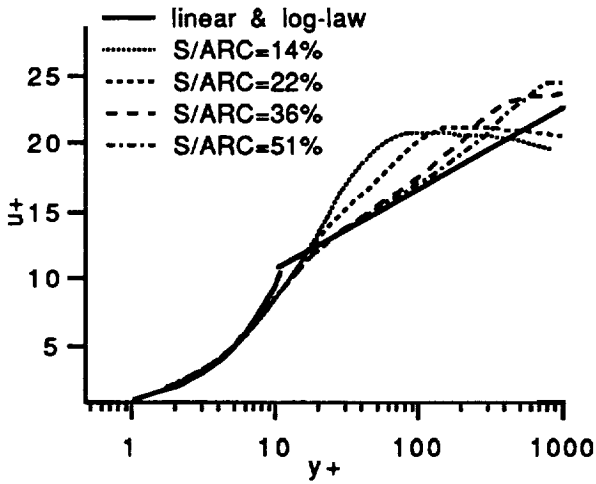


Fig. 5b Velocity profile along suction surface (LB)

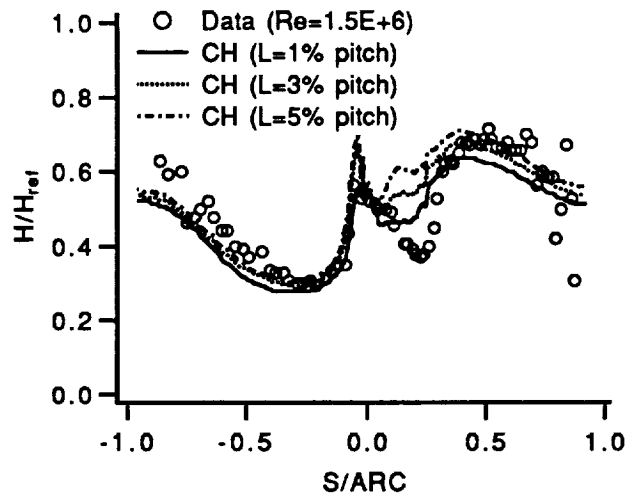


Fig. 8 Freestream turbulence length scale effect

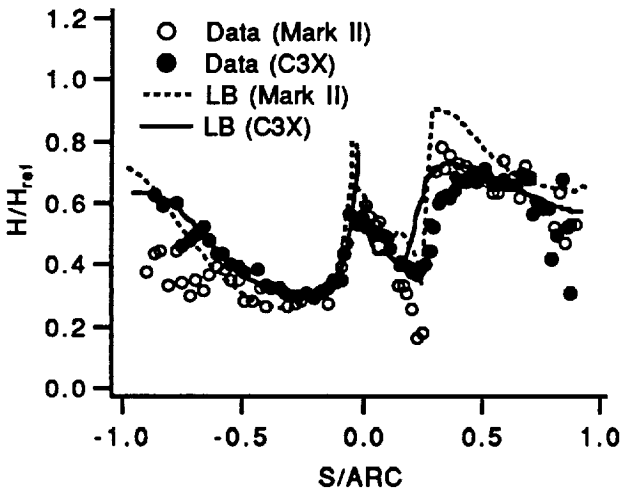


Fig. 6 Pressure gradient effect